Monetizing the role of water in sustaining watershed ecosystem services using a fully integrated subsurface–surface water model

Tariq Aziz[1,2,*], Steven K. Frey[1,3], David R. Lapen[4], Susan Preston[5], Hazen A. J. Russell[6], Omar Khader[1,7], Andre R. Erler[1], Edward A. Sudicky[1,3]

[1]Aquanty, 600 Weber St. N., Unit B, Waterloo, ON, N2V 1K4, Canada
[2]Ecohydrology Research Group, Water Institute and Department of Earth and Environmental Sciences, University of Waterloo, Waterloo, N2L 3G1, ON, Canada
[3]Department of Earth and Environmental Sciences, University of Waterloo, Waterloo, N2L 3G1, ON, Canada
[4]Agriculture and Agri-Food Canada, Ottawa Research and Development Centre, Ottawa, Ontario, Canada
[5]Environment and Climate Change Canada, Ottawa, Ontario, Canada
[6]Geological Survey of Canada, 601 Booth St., Ottawa, ON, K1A 0E8, Canada
[7]Department of Water and Water Structural Engineering, Zagazig University, AlSharqia, Egypt

[*]*Correspondence to*: Tariq Aziz (taziz@aquanty.com)

Abstract. Water is essential for all ecosystem services, yet a comprehensive assessment of total (overall) water contributions to ecosystem services production has never been attempted. Quantification of the many ecosystem services impacted by water demands integrated hydrological simulations that implicitly characterize subsurface and surface water exchange. In this study, we use a fully integrated hydrological model—HydroGeoSphere (HGS)—to capture changes in subsurface water, surface water, and evapotranspiration (green water) combined with the economic valuation approach to assess ecosystem services over an 18-year period (2000-2017) in a mixed-use but predominantly agricultural watershed in eastern Ontario, Canada. Using the green water volumes and ecosystem services values as inputs, we calculate the marginal productivity of water, which is \$0.45 per m^3 (in 2022 Canadian dollars). The valuation results show that maximum green water is used during the dry years, with a value of \$1.16 billion during a severe drought that struck in 2012. The average product of water for ecosystem services declines during the dry years. Because subsurface water is a major contributor to the green water supply, it plays a critical role in sustaining ecosystem services during drought conditions. For instance, during the 2012 drought, the subsurface water contribution to green water was estimated at \$743 million, making up 72% of the total value of green water used in that year. Conversely, the surface water contributions in green water provision over the modeling period are comparatively miniscule. This study informs watershed management on the sustainable use of subsurface water during droughts and provides an improved methodology for watershed-based integrated management of ecosystem services.

1 Introduction

The role of subsurface water (groundwater and soil water in the vadose zone) in socio-economic development is widely acknowledged (Foster and Chilton, 2003); its ecological contributions are, however, undervalued (Yang and Liu, 2020), despite being fundamental to the control of terrestrial ecological processes (Qiu et al., 2019). Subsurface water supports a potpourri of ecosystem services that range from provisioning to regulating, supporting, and cultural services (Griebler and Avramov, 2015). While water infiltration is a driver for subsurface water recharge, subsurface

36 water discharge is in-turn key for supporting terrestrial ecosystems (e.g., wetlands, forests, etc.) (Griebler and

37 Avramov, 2015). Hence, subsurface water provides a buffer against weather stressors on vegetation and aquatic

38 ecosystems and helps to maintain key processes that underpin ecosystem services (Qiu et al., 2019). To date, most

39 ecosystem services research has focused on aboveground factors and processes (e.g., land use change), and very little

40 focus has been given to the critical zone (e.g., shallow groundwater) and its influence on terrestrial ecosystem services

41 (Richardson and Kumar, 2017; Qiu et al., 2019). In a few instances, previous research (e.g., Booth et al., 2016; Li et

42 al., 2014) has attempted to link subsurface water with land cover, but only at a field scale and under static

43 environmental conditions (Qiu et al., 2019). Given the difficulties with mapping large/watershed scale subsurface

44 water resources, the contribution of subsurface water towards terrestrial ecosystem services has rarely been quantified.

45 Furthermore, monetary/economic valuation of subsurface water contribution to terrestrial ecosystem services has

46 never been attempted.

47 While hydrologic ecosystem services studies are common in the literature (Ochoa and Urbina-Cardona, 2017),

48 groundwater-focused ecosystem services assessments have rarely been undertaken. However, groundwater can be an

49 important regulator of watershed hydrologic behavior and ecosystem health, especially in regions with a shallow water

50 table, such as the Great Lakes Basin (Neff et al., 2005). In addition, the groundwater acts as a soil water source in

51 areas of shallow water table (Chen and Hu, 2004). The importance of groundwater has been noted by Griebler and

52 Avramov (2015) in their review of groundwater ecosystem services, where they highlight that groundwater plays a

53 direct role in supplying different types of ecosystem services (Millenium Ecosystem Assessment (MEA), 2005); and

54 they stress the need for a better quantitative understanding of groundwater processes in order to protect and manage

55 groundwater ecosystem services. Furthermore, Mammola et al. (2019) emphasize that subterranean ecosystems are

56 largely being overlooked in conservation policies. Based on a preliminary assessment of all the regions around the

57 world where groundwater plays a critical role in ecosystem services (considering that 43 % of consumptive irrigation

58 is sourced from groundwater (Siebert et al., 2010)), one has to wonder if the lack of focus on subsurface water

59 ecosystem services is not due to lack of need, but in fact a lack of tools with which to conduct the required analysis.

60 Using advanced hydrological models is a convenient approach to completely characterize all water storage and flux

61 dynamics over large spatial scales. With groundwater ecosystem services' increasing role in policy-making (Honeck

62 et al., 2021) and sustainable groundwater resources management, additional tools are required in order to map them

63 more accurately. At present, numerous modeling tools are available for ecosystem services mapping, such as

64   ARtificial Intelligence for Environment & Sustainability (ARIES), Co$ting Nature, Envision, and Integrated

65   Valuation of Ecosystem Services and Tradeoffs (InVEST), with InVEST being by far the most prominent in the

66   scientific literature (Ochoa and Urbina-Cardona, 2017). The only approach to completely characterize all water storage

67   and flux dynamics over large spatial scales is through the use of sophisticated hydrological models. For mapping

68   hydrological ecosystem services, it is essential to understand and capture complex hydrological processes (Sun et al.,

69   2017). However, ecosystem services specific models, such as the InVEST Water Yield Model, have limited capability

70   to simulate hydrological processes efficiently (Redhead et al. 2016). The hydrologic tools built into the ecosystem

71   services models are usually focused on one water compartment and/or are too simplistic to properly characterize

72   hydrologically mediated ecosystem services (Dennedy-Frank et al., 2016; Vigerstol and Aukema, 2011). Still, models

73   like SWAT and many other hydrological models, such as Variable Infiltration Capacity (VIC) and Finite Element

74   subsurface FLOW (FEFLOW) models, are unable to simulate integrated subsurface-surface water systems. Within

75   the hydrologic modelling community, it is acknowledged that structurally complex, fully-integrated subsurface–

76   surface water models are the current state-of-the-art for capturing the interplay between subsurface and surface water

77   systems, however, this class of models has not yet been applied towards ecosystem services valuation.

78   Another key hydrological and ecological process is evapotranspiration, which can be largely supported by the

79   availability of groundwater (Jin et al., 2017; Condon et al., 2020). Changes in evapotranspiration rates determine water

80   availability and ecosystem health at a watershed scale (Zhao et al., 2022). Thus, subsurface water availability is vital

81   for ecosystem functioning and subsequent ecosystem services. Under drought conditions, subsurface water can

82   become critically important for sustaining evapotranspiration (Condon et al., 2020). Therefore, mapping the

83   connection between subsurface water and evapotranspiration is imperative for sustainable water and ecosystem

84   services management (Yang et al., 2015), especially in cases where growing climate variability is expected to result

85   in increasingly erratic precipitation patterns (Taylor et al., 2013). A few of the current hydrological models can weakly

86   capture the subsurface water dynamics and subsurface-surface water interactions (Clark et al., 2015). Because

87   HydroGeoSphere (HGS) is an integrated subsurface-surface model, it can be used to dynamically integrate key

88   components of the terrestrial hydrologic cycle such as evaporation from bare soil and water bodies, vegetation-

89   dependent transpiration with root uptake, snowmelt and soil freeze/thaw dynamics.

90   Evapotranspiration represents large fluxes of both water and energy across the land surface–atmosphere boundary and

91   is closely related to terrestrial ecosystem production (Tan et al., 2021). Water managers perceive evapotranspiration

92   as a water loss; however, it is an essential process for regulating the hydrologic cycle and providing terrestrial

93   ecosystem services (An and Verhoeven, 2019). Evapotranspiration is also called green water—the fraction of the

94   rainfall on the land that eventually returns to the atmosphere as evapotranspiration—which is a source of nutrition for

95   vegetation/ecosystems and plays a key role in producing ecosystem services (Zisopoulou et al., 2022; Schyns et al.,

96   2019).   Green water is evapotranspired during biomass production, and thus supports and maintains terrestrial

97   ecosystems (Lowe et al., 2022). Hence, evapotranspiration is pivotal in the growth and functioning of ecosystems (Liu

98   and El-Kassaby, 2017) and plays a major role in providing ecosystem services through biomass production. It is also

99   a key process by which to model/map terrestrial ecosystem services production. To capture the interaction between

100   evapotranspiration and subsurface and surface waters, fully-integrated subsurface–surface water models are well

101   suited.

102   In this study, we introduce the HydroGeoSphere (HGS), a fully-integrated subsurface– surface water model, as a tool

103   for mapping and quantifying subsurface and surface water contributions to terrestrial ecosystem services at the

104   watershed scale (~4000 km^2). Furthermore, the results from the HGS modelling are extended to an economic valuation

105   of water contributions to ecosystem services. Until now, fully integrated subsurface-surface models such as HGS have

106   not been demonstrated in the scientific literature as tools for modeling ecosystem services, and the economic value of

107   subsurface water has been overlooked in ecosystem services valuation assessments. To address this omission, we

108   demonstrate the model for a watershed in a humid temperate climate in eastern Ontario, Canada, with a generally

109   shallow (1-3m) water table. Furthermore, using the simulation results, we value the contribution of subsurface and

110   surface water storages to evapotranspiration and subsequently to terrestrial ecosystem services. As such, the work

111   herein provides an important and novel contribution to the science of ecosystem service valuation in terms of both

112   conceptual and methodological understanding. This work identifies the level of complexity required in a model to

113   quantify water ecosystem services, especially from shallow water regions.

2 Materials and Methods

2.1 Study Area

116   The South Nation watershed (SNW), located in eastern Ontario, Canada, covers approximately 3,830 km^2 (Fig. 1).

117   There is approximately 100 m of vertical relief in the land surface, and the relief is relatively flat (Fig. 1A). It is

118   primarily an agriculture-focused watershed, with relatively low population density. The towns of Casselman, Russell,

119   and Winchester have respective populations of 3,548, 16,520 and 2,394 based on the 2016 Canada census. The eastern

120   flank of the city of Ottawa is encroaching on the Northwest corner of the watershed, in many headwater areas. The

121   SNW stream network is approximately 6,489 km long and consists of 1,606 km of Strahler order 3+, 1,548 km of

122   Strahler order 2, and 3,335 km of Strahler order 1 features (Fig. 2A). Many of the low order features are either

123   completely manmade agricultural drainage ditches, or straightened natural watercourses designed to drain the

124   agricultural landscape.

125   Soil drainage conditions across the watershed are primarily imperfect, poor, or very poor (Fig. 3A), although some

126   disconnected pockets are considered well drained (SLC, 2010). The wide extent of poorly drained soils in the SNW

127   is an integral reason for the intensive land drainage activities. Tile drainage is extensively employed to enhance

128   agricultural productivity and to facilitate cropping activities in these soils. Approximately 960 km^2 (or 25 %) of the

129   watershed is tile-drained (Fig. 4A). From 2004 to 2016, 290 km^2 of land was tile drained. Across most of the SNW,

130   the soils are underlain by Quaternary deposits, primarily of glacial, glacial marine, fluvial, and colluvial origin

131   (Ontario Geological Survey, 2010). These sediments are composed of sand, silt, clay, gravel, and glacial till, and range

132   in thickness from 0 m to approximately 90 m across the watershed. Eight soils have been identified in the SNW (SLC,

133   2010), mainly composed of clay loam and sandy loam textures (Fig. 3A(a)). Localized areas associated with incised

134   bedrock channels and Quaternary esker deposits are important sources of groundwater for both ecological function

135   and human/livestock supply, and most of the rural residents in the SNW rely on groundwater for domestic and farm

136   use.

137   The SNW is characterized by relatively wet temperate climate with ample amounts of snow in winter and warm

138   summers. The annual average temperature is just over 5 C, with average summer highs reaching 26°C in July and

139   average winter lows reaching -14°C in January (https://climate.weather.gc.ca/climate_normals). Present day

140   landcover (Fig. 1) consists of 38% cropland, 29% forest, 20% grassland, 7% urban, 5% wetland, and 1% water. The

141   dairy industry is a big part of the SNW economy, and the grassland areas provide grazing area to feed the cattle.

142
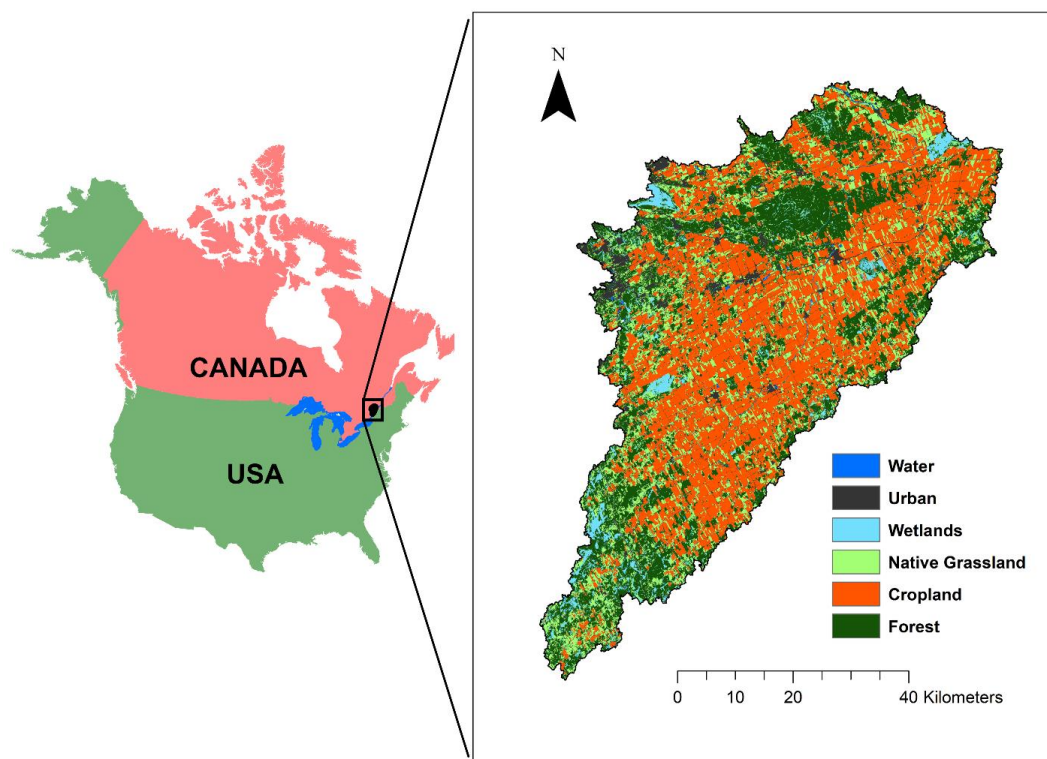
Figure 1: Location of the South Nation Watershed (SNW) in North America. The figure in the inset (right) shows the

land use types in the SNW.

2.2 Capturing changes in water storages using HGS Model

As HGS is a fully integrated model, it generates simulation outputs for all components of the terrestrial hydrologic

cycle (Fig. 2) in a completely transient format, thus alleviating a common limitation of ecosystem services models in

that they do not account for transient behavior (Vigerstol and Aukema, 2011). Furthermore, HGS outputs can also be

generated for the entire model domain (i.e., the watershed) or refined for smaller spatial scales such as subwatersheds,

with the downscale limit being that of an individual finite element within the Finite Element Method (FEM).

A - Surface Water Flow   B - Surface Runoff
C - Wetland Water Storage D - Groundwater Discharge
E - Groundwater Recharge   F - Regional Aquifer Level
G - Water Table Position   H - Soil Moisture Level
I - Tile Drain Discharge   J - Evapotranspiration

151
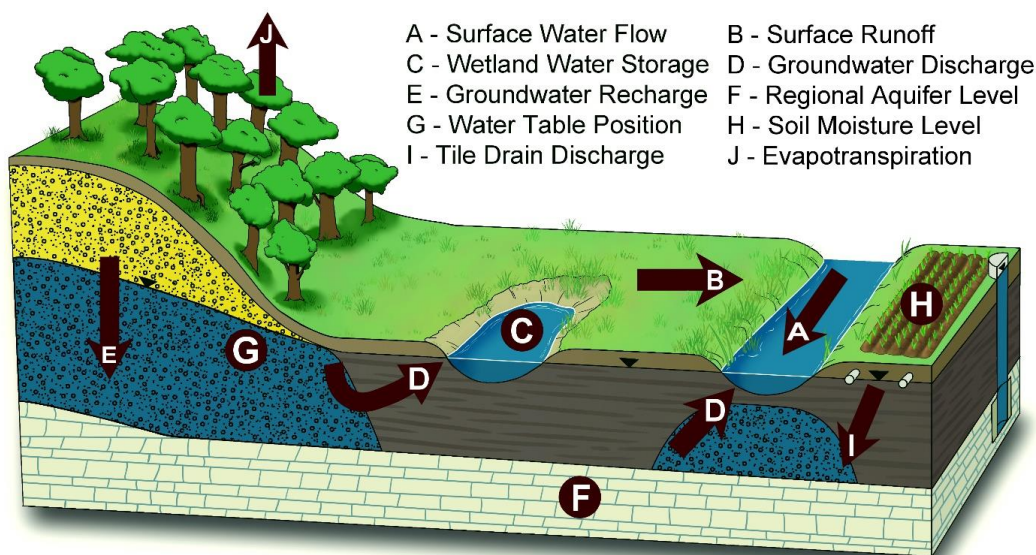
152   Figure 2: Key components of terrestrial hydrological cycle mapped by the HGS model

153   However, it should be noted that the integrity of the HGS outputs are also dependent on the model scale, in that, for

154   example, a model of a 150,000 km^2 river basin is best suited to answer big picture questions (i.e., basin water balance,

155   climate change impacts, regional groundwater), while a model built for the SNW can be used to address questions

156   pertaining to localized processes (i.e., individual wetland influences, groundwater recharge and discharge patterns,

157   flood extent, local aquifer conditions, local soil moisture conditions). If even more localized insights are required,

158   HGS models can be resolved down to field or plot scale, where highly detailed questions pertaining to things such as

159   riparian zones, soil structure, manure application, and tile drainage influences on water quantity and quality can be

160   evaluated. However, for field or plot scale insights, the model domain typically would be no larger than $10 - 20$ km^2.

161   Thus, HGS is a scalable and robust model. We use the model to capture watershed surface water outflow, actual

162   evapotranspiration (ET$_a$) (which are correlated to biomass production), subsurface water storage, and land surface

163   water storage (reflective of how much water is held in wetlands and reservoirs).

164   **2.2.1 Model construction**

165   **2.2.1.1 Finite Element Mesh (FEM)**

166   The HGS model utilizes a 3-D unstructured finite element mesh (FEM) that extends across the full 3830 km^2 area of

167   the SNW. Within the structure of the FEM are 1-D river/stream channel features, a 2-D overland flow domain

168   (reflecting land surface topography), and a 3-D subsurface flow domain (reflecting hydrostratigraphy). The FEM for

169   the SNW model resolves all Strahler 2+ stream/river features as control lines in the mesh. FEM node spacing (element

170   edge length) was maintained at 100 m along the control lines, while away from the control lines the node spacing

171   extends up to 300 m. On each FEM layer there is a total of 86,740 nodes and 171,609 finite elements. Accordingly,

172   over the eight subsurface mesh sheets (seven subsurface layers); the FEM contains 693,920 nodes and 1,201,263 3-D

173   finite elements. In addition, the surface layer contains an additional 86,740 nodes and 171,609 2-D finite elements.

174   **2.2.1.2 Hydrostratigraphy**

175   The seven subsurface layers represent (from the top down) three soil layers, three Quaternary geology layers, and one

176   bedrock layer. The soil layers extend from 0–0.25 m, 0.25–0.5 m, and 0.5–1 m depth relative to the top surface, which

177   is defined using the Ontario Integrated Hydrology digital elevation model (Ontario Integrated Hydrology Data:

178   Elevation and mapped water features for provincial scale hydrology applications). The hydraulic properties for the

179   soil layers vary spatially according to the soil polygons defined in the Soil Landscapes of Canada (SLC, Soil

180   Landscapes of Canada Working Group, 2010), and are defined in two steps as follows: (1) properties extracted from

181   SLC are used in conjunction with the Rosetta pedotransfer functions (Schaap et al., 2001) to obtain estimates for

182   hydraulic conductivity, water retention and relative permeability, residual saturation, and porosity parameters, and (2)

183   hydraulic conductivity, water retention and relative permeability parameters are manually tuned during model

184   calibration. The three Quaternary layers are of variable thickness, where the layer interfaces represent contrasting

185   lithology using a simplified version of the 3-D geological model produced by Logan et al., (2009). Hydraulic

186   properties for the Quaternary materials are assigned based on lithology. Underlying the Quaternary layers is a single

187   layer of uniform hydraulic conductivity representative of the Phanerozoic bedrock. When assembled, the model layers

188   depict a 3-D subsurface realization of the SNW hydrostratigraphy (Fig. 3).
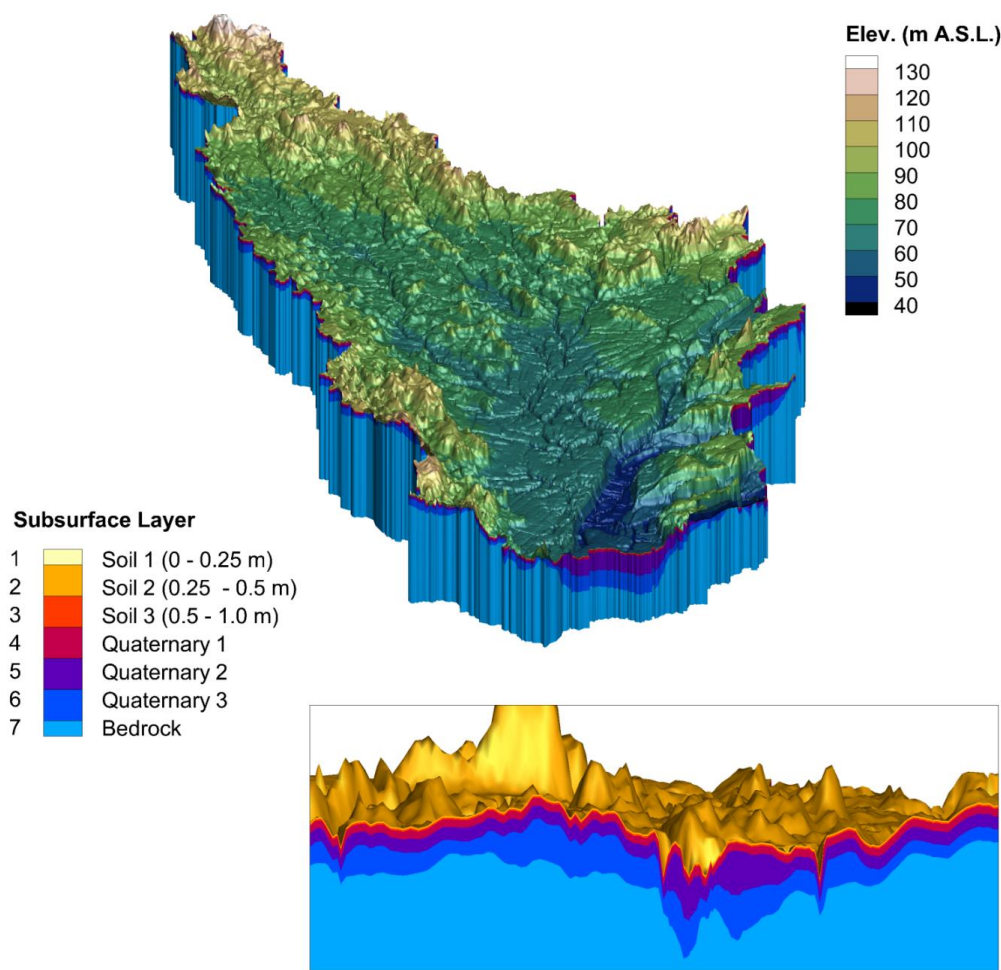
189

190   Figure 3: Three-dimensional perspective of the South Nation HydroGeoSphere model, and the hydrostratigraphic

191   layering (inset). Note the 100x vertical exaggeration.

192   **2.2.1.3 Land Surface Configuration**

193   The land surface in the HGS model represents land cover distribution defined by the gridded, 30 m resolution, 2017

194   Annual Crop Inventory dataset (Annual Space-Based Crop Inventory for Canada, 2017), that is refined to six

195   categories (water, urban, wetland, grassland, cropland, and forest). Root depth for the cropland (1 m), forest (2.9 m),

196   wetland (1 m), grassland (2.1 m), and urban (1 m) landcovers was held static over the simulation interval. Spatially

197   distributed leaf area index (LAI) is a transient parameter represented by the 8-day composite, 500 m resolution

198   MOD15A2H v006 data product (MYD15A2H MODIS/Aqua Leaf Area Index/FPAR 8-Day L4 Global 500m SIN

199   Grid. NASA LP DAAC). Each landcover category also utilized a unique value for surface roughness (Manning's n

200   coefficient), ranging from 0.001 (urban) to 0.03 s/m$^{1/3}$ (forest).

2.2.1.4 Climatology

202   Time-varying and spatially distributed climate data with daily temporal resolution is used as forcing for the liquid

203   water influx (LWF) and potential evapotranspiration (PET) boundary conditions in the HGS model for the 2000 to

204   2018 simulation interval. LWF is derived from precipitation obtained from McKenney et al. (2011) in combination

205   with snow water equivalent (SWE) estimates from the ERA5-Land land-surface reanalysis (Muñoz-Sabater et al.,

206   2021), where LWF is the sum of liquid precipitation (rain) and snowmelt (daily changes in SWE).

207   Potential evapotranspiration (PET) is used to calculate ET$_a$ within HGS. PET primarily depends on the surface

208   radiation budget, temperature, humidity, and near-surface wind speed (Allen et al., 1998); however, out of these

209   variables, only minimum and maximum temperature are readily available for the full SNW. Hence, PET forcing for

210   the SNW model is calculated with the Hogg method (Hogg, 1997). This is consistent with Erler et al. (2019) and Xu

211   et al. (2021), who reported good agreement with the observed water balance in the Great Lakes region when using the

212   Hogg method. The Hogg method is based on the FAO Penman-Monteith approach (Allen et al. 1998), where the

213   radiation budget and humidity are approximated as a function of daily minimum and maximum temperature (and wind

214   is assumed to be constant).

2.2.2 Model Performance Evaluation

216   The performance of the SNW HGS model is evaluated using observed surface water flow rates and groundwater levels

217   from across the watershed. The observation data is derived from surface water flow monitoring conducted at 9 Water

218   Survey of Canada (WSC) hydrometric stations (Figure 4a) and 10 Provincial Groundwater Monitoring Network wells

219   (Figure 4b). The Nash-Sutcliffe Efficiency (NSE) and Percent Bias (Pbias) metrics (Moriasi et al., 2007) are used to

220   evaluate surface water flow simulation performance, while the coefficient of determination (R^2) is used to evaluate

221   groundwater simulation performance.
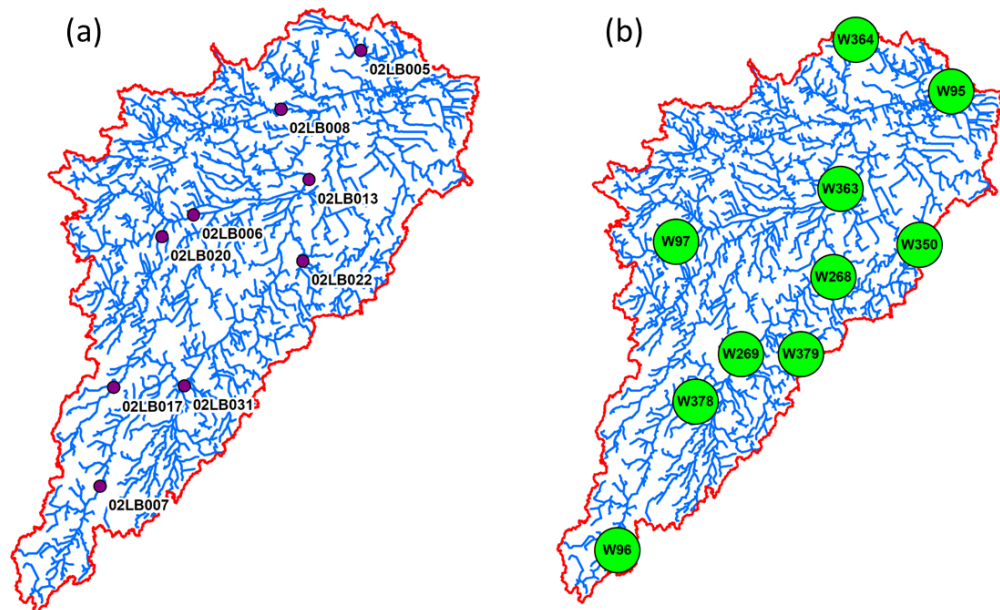
Figure 4. Distribution of (a) Water Survey of Canada surface water flow gauges, and (b) Provincial Groundwater Monitoring Network wells across the South Nation watershed.

2.3 Ecosystem services water productivity

We use the benefit transfer method to derive the unit values of ecosystems in the SNW. The value transfer method, which is a widely used and quick technique for assessing the economic value of ecosystem services, relies on secondary data obtained through the implementation of various other economic valuation methods (Aziz, 2021). A local study by L'Ecuyer-Sauvageau et al. (2021) assembles the values for 13 ecosystem services: agricultural services, global climate regulation, air quality, water provision, waste treatment, erosion control, pollination, habitat for biodiversity, natural hazard prevention, pest management, nutrient cycling, landscape aesthetics, and recreational activities. Because of unavailability of data, raw material, genetic diversity, spiritual, cultural and heritage identity services are excluded from the analysis. These unit values have been correspondingly generated by major ecosystems in the adjacent Ottawa-Gatineau region using market price, replacement cost, and benefit transfer methods. The unit values for ecosystem services are gathered based on similarities of ecologic and socio-economic conditions between the studied and policy sites, and converted using the purchasing power parity (L'Ecuyer-Sauvageau et al., 2021). After

237 adjusting these values for inflation, we calculate the value of ecosystem services in the SNW for the simulation period

238 using the following equation.

239
$$EV_t = \sum_{k=1}^{n}(A_k \times UV_k) * VI \qquad (1)$$

240 A_k= Area of land use k

241 UV_k= Unit value of ecosystem services for land use k

242 VI= Vegetation indicator, a ratio of yearly to average net primary production=NPP_{year}/NPP_{mean}

243 We use net primary production as an indicator to characterize the vegetation vigor (Xu et al., 2012) and to adjust the

244 values of ecosystem services over time in the SNW. The relative vegetation indicator (VI) is the ratio of yearly NPP

245 and the mean NPP over the selected period. The Moderate Resolution Imaging Spectroradiometer (MODIS) data

246 (https://appeears.earthdatacloud.nasa.gov/) for NPP (at 500m resolution) is collected from 2000 to 2017. Using the

247 spatial analyst tool of ArcGIS and raster data for NPP, we calculate yearly mean values of NPP over the selected time

248 period. The average NPP values from 2000-2017 for the SNW are given in Table 1.

249 We then calculate the average ecosystem services water productivity using ecosystem services values and green water

250 volumes in equation 2:

251
$$V_W = (EV_t)/(X_w) \qquad (2)$$

252 V_w is the average product of water ($ per m^3), X_w is the total volume of ET_a/green water used in a year 't'.

253 **2.4 Valuation of subsurface water contribution towards ecosystem services supply**

254 Firstly, we develop a water production function for ecosystem services supply using total values of the watershed over

255 the 18-year period and corresponding volumes of green water consumed. Because ecosystem services value is

256 proportional to biomass production (Costanza et al., 1998), the values are modified over the time using relative

257 changes in biomass of ecosystems in the watershed (Xu and Xiao, 2022). The slope of the production function

258 represents the ecosystem services marginal water productivity (MP_w). Secondly, the HGS model captures the volumes

259 of subsurface and surface water used in supporting ET_a. Using the volumes of storages consumed for ET_a and MP_w,

260 the economic value of storages is calculated for ecosystem services supply (Eq.3).

261
$$V_i = X_{wi} * MP_w \qquad (3)$$

262 Where V_i is the value of water storage i towards ecosystem services supply, X_{wi} is the volume of water storage i used

263 towards green water supply, MP_w is the marginal productivity of water.

264 **3 Results**

265 **3.1 HGS outputs**

266 For the 2000 to 2018 simulation interval, the HGS model is able to reproduce surface water flow rates at the nine

267 WSC hydrometric stations across the SNW with good accuracy. Based on daily evaluation frequency, NSE ranged

268 from 0.59 to 0.70, with a mean of 0.66; while PBias ranged from -17.4 % to 17.1 %, with a mean of 3.9 %. Groundwater

269 levels were also reproduced across the SNW with reasonable accuracy for the 2000 to 2018 interval. The R^2 between

270 simulated and observed water levels in the 10 observation wells is 0.98, with the simulated values having a mean value

271 2.8 m higher than the observed values.

272 HGS outputs (Fig. 5) represent conditions associated with continuous simulation of the SNW over 2000 to 2017 time

273 interval, and the calibration metrics are also based over the same time interval. Included are watershed surface water

274 outflow, ET_a rates (which are correlated to biomass production), subsurface water storage (groundwater storage plus

275 soil moisture storage) and land surface water storage. These storage zones recharge and discharge over time, but the

276 biggest dip is shown in 2012—the drought year.
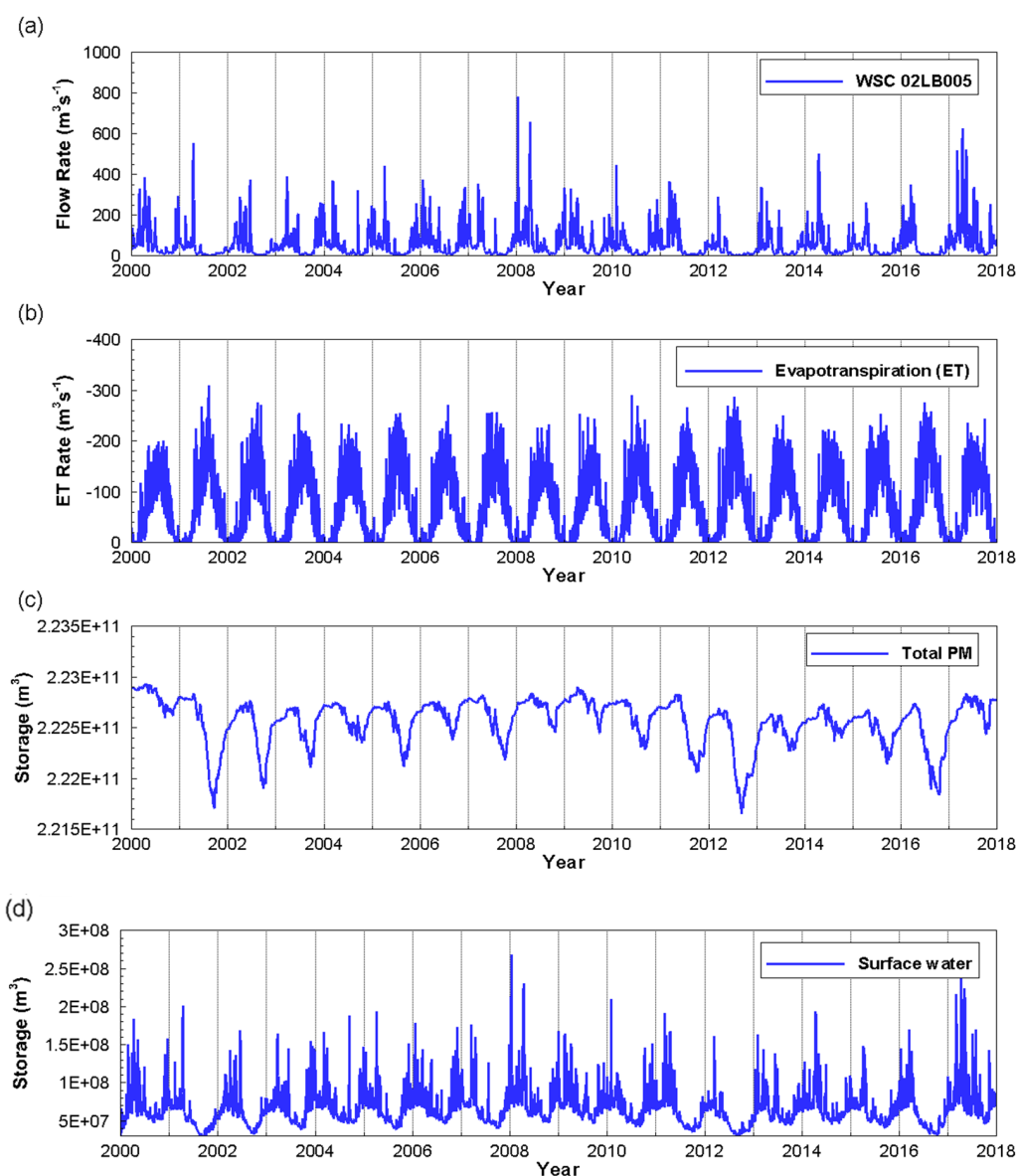
Figure 5: Time series outputs from the South Nation watershed HydroGeoSphere (HGS) simulation over the 2003-to-2018-time interval. (a) stream flow at a representative gauge location, (b) watershed evapotranspiration, (c) watershed subsurface water storage, and (d) watershed land surface water storage.

We aggregate the daily values to yearly values to counter the lag affects. The numeric data for the variables presented in Fig. 5 is given in the Table 1A. The mean change is calculated to analyze the fluctuations in the storages over time

283   (Fig. 6). The year 2012 (the drought year) shows the maximum increase in evapotranspiration and a high dip in the

284   subsurface water storage.

285
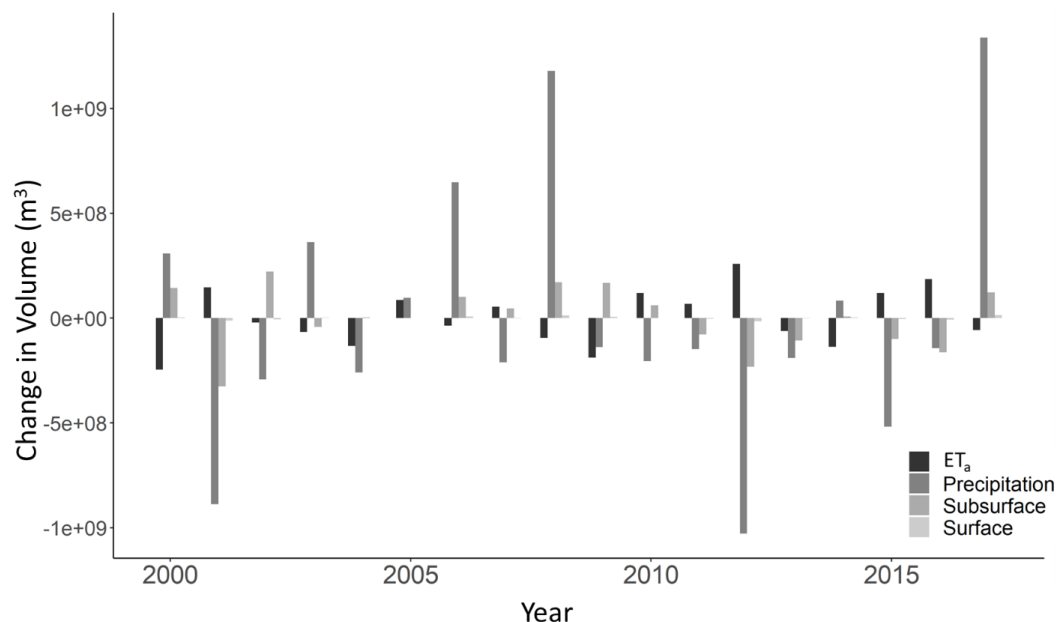
286   Figure 6: Mean changes in surface and subsurface water storages, ET_a, and precipitation over time

287   **3.2 Valuation of ecosystem services, and average and marginal water productivity**

288   The unit values developed for major land use types in the SNW are given in table 1

289   Table 1: Land use types and unit values for the SNW

Land Use	Area (hectare)	Unit value ($/hectare/year)
Water	1,299	165
Urban	25,734	1,177
Wetlands	16,709	71,273
Native Grasslands	7,6961	4,152
Croplands	154,810	1,666
Forest	107,470	4,993

290

291   Using the unit values (Table 1) and land use area, we calculate a total value of $2.33 billion per year for 13 ecosystem

292   services in the SNW and the value is further modified for each year using the NPP values in Eq. 2. The estimates for

293   average product of water are point estimates for each year based on the value of ecosystem services and green water

294   volume for the corresponding year. The NPP data, ES values, ET_a and average water product in the SNW for each

295   year are given in the Table 2.

296   Table 2: Mean NPP, ecosystem services (ES) values and average water product for the SNW from 2000 to 2017

Year	Mean NPP (Kg C/m²/year)	ES Value (x10⁹ $/year)	ET_a (x10⁹ m³)	Average product of water ($/m³)
2000	0.59	2.26	2.09	1.08
2001	0.65	2.49	2.48	1.00
2002	0.6	2.30	2.31	0.99
2003	0.6	2.30	2.26	1.01
2004	0.62	2.37	2.20	1.08
2005	0.63	2.41	2.42	1.00
2006	0.58	2.22	2.29	0.97
2007	0.63	2.41	2.39	1.01
2008	0.6	2.30	2.24	1.03
2009	0.58	2.22	2.14	1.04
2010	0.64	2.45	2.45	1.00
2011	0.6	2.30	2.40	0.96
2012	0.63	2.41	2.59	0.93
2013	0.58	2.22	2.27	0.98
2014	0.59	2.26	2.19	1.03
2015	0.65	2.49	2.45	1.02
2016	0.6	2.30	2.52	0.91
2017	0.59	2.26	2.27	0.99

297   For the ecosystem services marginal water productivity, we develop a production function using ET_a and ES values

298   for the SNW (Fig. 7). The slope of the production function is marginal productivity of water, which is $0.45/m³ in the

299   SNW.
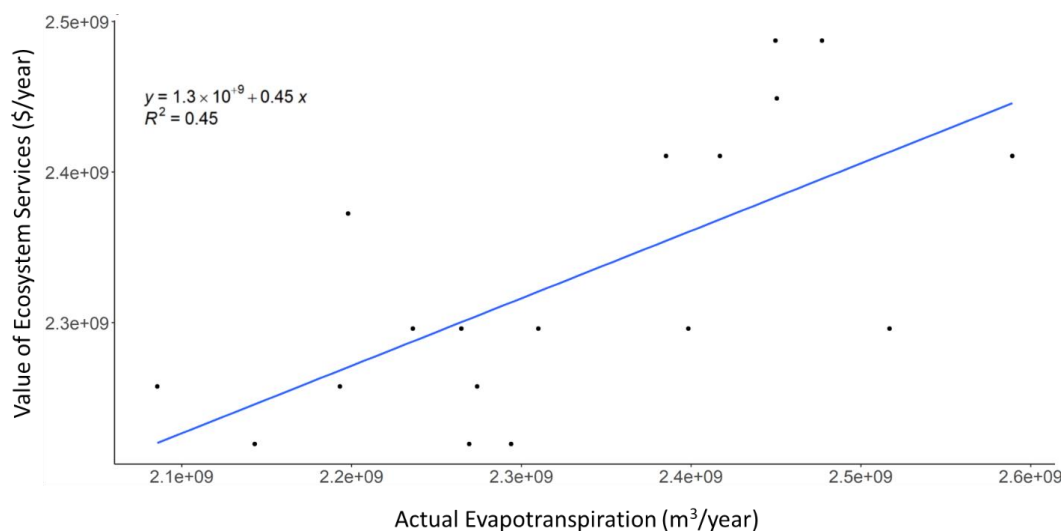
300

301   Figure 7: Ecosystem services water production function in the SNW

302   To assess the contribution of subsurface water towards ecosystem services, we calculate the average ecosystem

303   services water productivity at the watershed scale. The average product of water over the modeling period of 18 years

304   ranges from \$0.91-1.08 per m^3 (Fig. 8). During the drought periods (years 2001, 2012 and 2016), the average product

305   of water declines and is minimum. The average product shows efficiency in use of water across the modeling period.

306   It is the maximum for year 2000, meaning the conditions (other variables like precipitation) were favoring the

307   maximum production of ecosystem services with the lowest water consumption in that year.
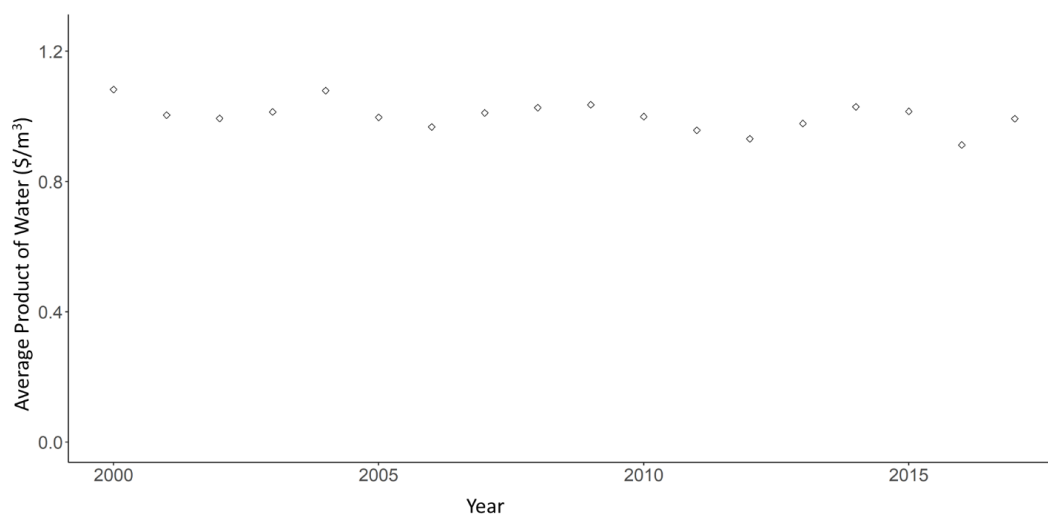
308

309 Figure 8: Average product of water for ecosystem services in the SNW

310 **3.3 Valuation of green, subsurface, and surface waters**

311 Using the marginal water productivity and ET_a in the SNW, we calculate the value of green water over the modelling

312 period (Fig. 9).
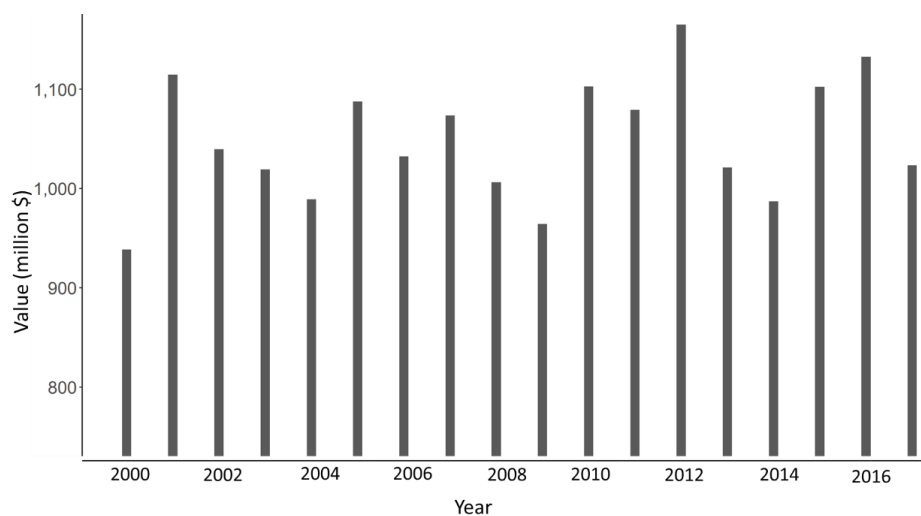
313

314 Figure 9: Value of green water in the SNW

315   We use the subsurface water evapotranspiration and surface water evaporation to calculate the contribution of these

316   two storages towards ET_a. Finally, these contributions in terms of water volume are valued using the marginal value

317   of water to account for subsurface and surface water inputs to the green water supply.

318
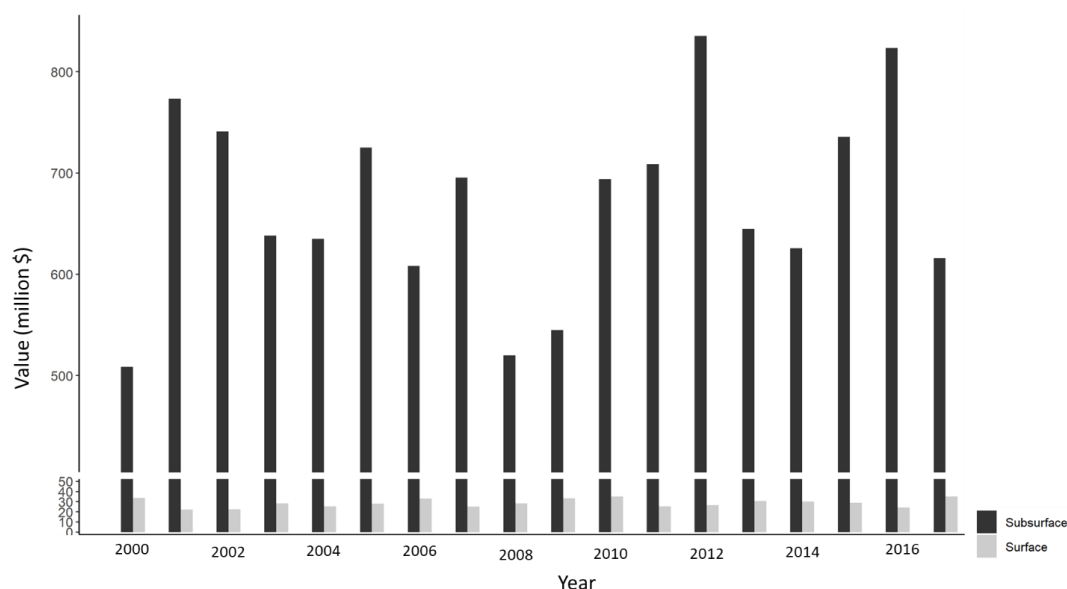
319   Figure 10: Contribution of subsurface and surface water towards green water supply in the SNW. (Note the break in

320   y-axis from 50 to 500)

321   **4 Discussion**

322   ET_a is a key phenomenon that sustains terrestrial ecosystem functions such as biomass production, and thus helps to

323   supply a variety of ecosystem services. As a fully integrated model, HGS generates simulation outputs for all

324   components of the terrestrial hydrologic cycle in a completely transient format, thus alleviating a common limitation

325   of most water models in that they do not account for transient behavior (Vigerstol and Aukema, 2011). We use HGS

326   to capture fluctuations in subsurface water and surface water storages, which can be used to quantify the role of these

327   storages in sustaining ET_a and subsequent ecosystem services. Then we compute the change in these zones with respect

328   to mean storage. Our modelling results show that ET_a is mainly supported by subsurface water storage/fluctuations

329   with respect to magnitude/quantity of water consumed.

330   To further compare the fluctuations in different storage zones on a common scale, we compute the standard scores

331   (that is, the change in a storage/standard deviation) for each zone over time (Fig. 11). The standard scores show that

332   ET_a is supported by both surface and subsurface water storages during the drought periods. However, the contribution

333   of subsurface water by volume during dry periods is much bigger than that of surface water. That is, the subsurface

334   water shores up the surface water during droughts.

335
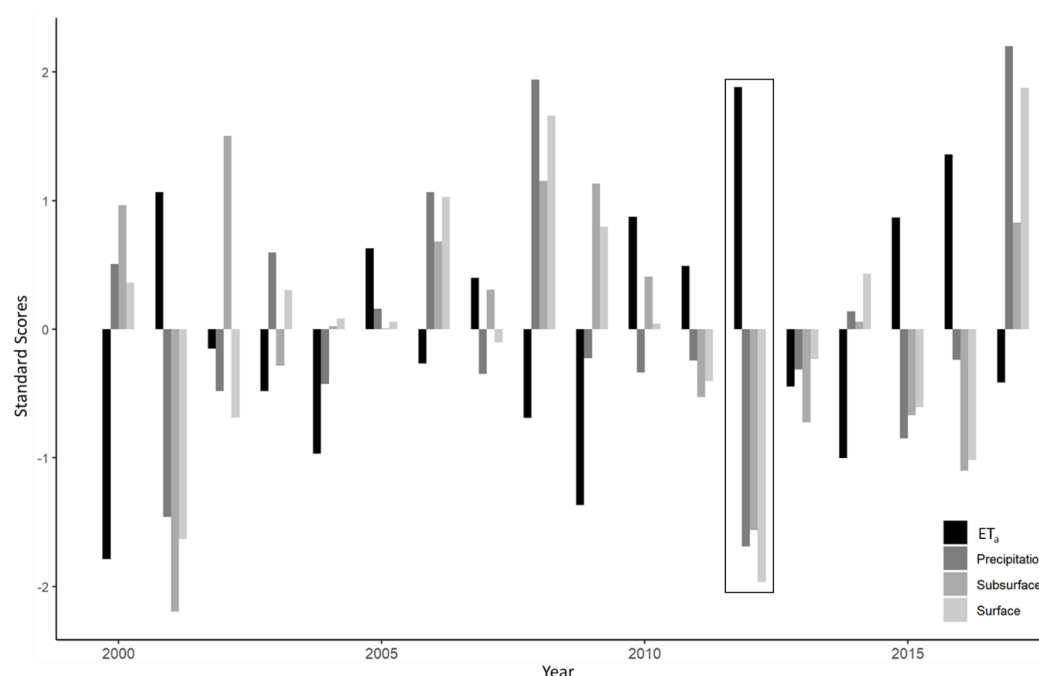
Figure 11: Change in standard scores of water storages/hydrological variables over the modeling period. The scores

337   for an anomaly year (2012) are bordered.

338   The comparison of years 2001 and 2012 (with less precipitation than mean) shows that the ET_a was less but outflow

339   was more in year 2001 than in 2012 (Fig. 5(a)). Thus, the drawdown in subsurface water in 2001 maintained the flows

340   in water bodies and streams in the watershed. The different response of subsurface water to two droughts (in years

341   2001 and 2012) in the watershed depends on the amounts of precipitation and other climatic conditions (e.g.,

342   temperature, atmospheric moisture demand, etc.) in the corresponding years (Zhao et al., 2022). During drought

343   periods, water demand for ET_a increases in most parts of the world due to high atmospheric moisture demand, resulting

344   in ecosystem stress and depletion of (subsurface and surface) water storages (Zhao et al., 2022). Similar to worldwide

345   trends described in Zhao et al. (2022), the ET_a rates in our study increase during dry periods. Given the complexities

346   involved in linking ET_a with surface and subsurface water storages, the impact of variations in ET_a rates on ecosystem

347   services during droughts remains unknown.

348   Our study is seminal in capturing the ecosystem services values with changing water supply/balance in a watershed

349   over a period of time. Few studies in the literature (e.g., Loheide, 2008; Su et al., 2022) have only estimated

350   groundwater evapotranspiration by linking water table fluctuation and changes in evapotranspiration. However, given

351   the flow of groundwater to soil vadose zone and surface water bodies, this approach of using water table fluctuations

352   is unable to yield accurate estimation of groundwater contribution towards sustaining evapotranspiration. The more

353   sophisticated HGS approach, by computing the subsurface water evaporation and transpiration, and surface water

354   evaporation, can assess the connections between ET_a and water storages more robustly.

355   The fluctuations in storages show that, in general, subsurface water storage repletes when ET_a is negative and depletes

356   when ET_a is positive. The years 2001 and 2012, drought years, are anomalies: ET_a is relatively higher than during the

357   wet years (high precipitation). The ET_a in drought years was mainly supported by the drawdown (by volume) in the

358   subsurface water storage below the mean level. Fluctuations in the subsurface water storage across the 18 years are

359   consistent with the changes in the precipitation, that is with above-average precipitation, the subsurface water storage

360   increases and vice-versa. On the other hand, increase in ET_a leads to reduction in subsurface storage and vice-versa.

361   The maximum recharge in the subsurface water storage occurs in the year 2002, immediately following a 2001 severe

362   dry period (within a 100-year time span) (Wheaton et al., 2008); 2002 was a year with less than average precipitation.

363   In regards to the economic valuation of water components, green water mainly benefits people at local scales (by

364   supporting biomass and ecosystem services in the area) whereas the benefits of blue water are seen at a wider basin

365   scale (Falkenmark and Rockström, 2010). Incorporating green-blue water resources at a watershed scale helps

366   integrate the role of water in land use and other terrestrial ecosystem functions. Therefore, for better management of

367   regional water resources, the use of fine-grained models becomes imperative to valuate the contributions of major

368   inland water storages towards green water supply. We develop a water production function using total green water

369   volumes and total values of SNW for 13 ecosystem services: agricultural services (net benefits from the crops or

370   agricultural products), global climate regulation, air quality, water provision, waste treatment, erosion control,

371   pollination, habitat for biodiversity, natural hazard prevention, pest management, nutrient cycling, landscape

372   aesthetics, and recreational activities. The ecosystem water production function yields a marginal value of $ 0.45 per

373   m^3 of green water/ ET_a (Fig. 7). Globally, Lowe et al. (2022) estimated the average marginal product of water at

374    $0.083 per m^3 for crop production only. Additional ET$_a$ supplies ecosystem services at a constant rate; however,

375   because the linear segment has a positive vertical intercept, the average ecosystem services water productivity

376   decreases with increase in ET$_a$ as the slope of the ray from origin through a point on production function diminishes

377   (Wichelns, 2014). On one hand, the water productivity will be maximum at the smallest amount of water

378   used/consumed but, on the other hand, it will also produce the smallest value of ecosystem services in the watershed.

379   Higher amounts of water are evapotranspired in the drought years mainly due to drought-associated meteorological

380   conditions such as increase in temperatures (Zhao et al., 2022). However, NPP does not reduce during the drought

381   periods, a finding consistent with other studies on temperate watersheds (e.g., Hosen et al., 2019; Sun et al., 2016).

382   Our results show that the drought-induced water stress increases the ET$_a$ rates in the watershed, similar to Zhao et al.

383   (2022) and Diao et al. (2021). The increase in ET$_a$ associated with a little higher of NPP for drought years across the

384   modeling period lowers the ecosystem services water productivity during the dry periods in the watershed (Fig. 8).

385   In the SNW, more of green water is used during the dry years with less precipitation. Therefore, the green water has

386   a maximum value of $1,165 million for year 2012—a drought year (Fig. 9). In this value, the subsurface and surface

387   water contributions are $835.6 and $26.5 million, respectively (Fig. 10). The maximum contribution of the subsurface

388   water is also for the year 2012 and then in 2001, both drought years. Contrarily, the surface water contributes a

389   maximum of $35.2 million in year 2010—a relatively wet year. Because surface water availability declines during

390   droughts, its contribution towards green water supply diminishes. Over the 18-year modeling period in the SNW, the

391   subsurface water contribution towards green water supply varies from 52% to 73%, whereas surface water contribution

392   ranges from 2% to 3.6%. One reason that further adds to reduction in the surface contribution may be the tile drainage

393   in the watershed (Miller and Lyon, 2021). Nonetheless, the critical role that the subsurface water provides in sustaining

394   ecosystem services during dry periods in the watershed is evident.

395   Our methodology provides a basis for setting up a new model to assess the subsurface water contribution in other

396   places. The results and values used in the study are not transferable to other sites/watersheds. The marginal product

397   of water is a site-specific entity which will be different for other watersheds because both ecosystem services value

398   and ET$_a$ will change depending on land cover (mainly), NPP, precipitation, and soil types. Nevertheless, given the

399   dynamicity of the storages and their link to terrestrial ecosystem services, this valuation approach will yield reliable

400   results provided the entire methodology (modelling of water storages and ET$_a$, and valuation of ecosystem services)

401   is conducted accurately for other locations/sites/watersheds.

5 Conclusions

Subsurface water plays a key role in the supply of terrestrial ecosystem services. Until now, subsurface water has never been comprehensively valued for its contribution towards ecosystem services supply in a watershed. The primary impediment has been complexities involved in modeling of interdependencies in hydrologic fluxes such as connection between subsurface water discharge and green water use. Despite known connectivity, subsurface, land and atmosphere water storages were modeled independently prior to the introduction of fully integrated hydrologic models. In our work in the SNW, we take the innovative approach of using the HGS model and ecosystem services valuation technique to monetize the contributions of surface and subsurface waters to the green water supply over a period of 18 years (2000-2017). The results show that droughts are a major trigger to increase the green water use in the watershed. At the same time, a bigger portion of the green water is supplied by the subsurface water, ranging from 52% to 73% over the modeling period. The maximum green water value corresponded to year 2012 with severe drought conditions and equals $1,165 million. More importantly, 72% of the green water value during the drought comes from the subsurface water contribution. Similarly, in other dry periods, years 2001 and 2016, the subsurface contribution makes 69% and 73% of the total green water values, respectively. Thus, the subsurface water plays a key role in supplying green water and sustaining ecosystem services during critical periods in the watershed. This analysis can help in better managing and allocating the subsurface water resources under climate uncertainties at a watershed scale.

Author contribution

Tariq Aziz contributed to the project by developing the concept, methodology, formal analysis, investigation, and writing the original draft.

Steven K. Frey was involved in conceptualization, methodology, data curation, HGS modeling, project administration, and reviewing and editing the manuscript.

David R. Lapen contributed to the project by helping develop the methodology, reviewing and editing the manuscript, and assisting with project administration.

Susan Preston assisted with reviewing and editing the manuscript and project administration.

Hazen A. J. Russell was responsible for reviewing and editing the manuscript.

Omar Khader contributed to the project by working on HGS modeling.

Andre R. Erler was involved in data curation and reviewing the manuscript.

Edward A. Sudicky was responsible for project administration and reviewing the manuscript.

Declaration of interest

The authors declare that they have no known competing financial interests or personal relationships that could have appeared to influence the work reported in this paper.

References

Annual Space-Based Crop Inventory for Canada, 2017: https://open.canada.ca/data/en/dataset/32546f7b-55c2-481e-b300-83fc16054b95.

Allen, R. G., Pereira, L. S., Raes, D., and Smith, M.: Crop evapotranspiration guidelines for computing crop requirements, 1998.

An, S. and Verhoeven, J. T. A.: Wetlands: Ecosystem services, restoration and wise use, 325 pp., 2019.

Aziz, T.: Changes in land use and ecosystem services values in Pakistan, 1950–2050, Environ. Dev., 35, 1, https://doi.org/10.1016/j.envdev.2020.100576, 2021.

Booth, E. G., Zipper, S. C., Loheide, S. P., and Kucharik, C. J.: Is groundwater recharge always serving us well? Water supply provisioning, crop production, and flood attenuation in conflict in Wisconsin, USA, Ecosyst. Serv., 21, 153–165, 2016.

Chen, X. and Hu, Q.: Groundwater influences on soil moisture and surface evaporation, J. Hydrol., 297, 285–300, https://doi.org/10.1016/j.jhydrol.2004.04.019, 2004.

Clark, M. P., Fan, Y., Lawrence, D. M., Adam, J. C., Bolster, D., Gochis, D. J., Hooper, R. P., Kumar, M., Leung, L. R., Mackay, D. S., and Maxwell, R. M.: Hydrological partitioning in the critical zone: Recent advances and opportunities for developing transferable understanding of water cycle dynamics, Water Resour. Res., 1–28, https://doi.org/10.1002/2015WR017096.Received, 2015.

Condon, L. E., Atchley, A. L., and Maxwell, R. M.: Evapotranspiration depletes groundwater under warming over the contiguous United States, Nat. Commun., 11, https://doi.org/10.1038/s41467-020-14688-0, 2020.

Costanza, R., D'Arge, R., De Groot, R., Farber, S., Grasso, M., Hannon, B., Limburg, K., Naeem, S., O'Neill, R. V., Paruelo, J., Raskin, R. G., Sutton, P., and Van Den Belt, M.: The value of ecosystem services: Putting the issues in perspective, Ecol. Econ., 25, 67–72, https://doi.org/10.1016/S0921-8009(98)00019-6, 1998.

Dennedy-Frank, P. J., Muenich, R. L., Chaubey, I., and Ziv, G.: Comparing two tools for ecosystem service assessments regarding water resources decisions, J. Environ. Manage., 177, 331–340, https://doi.org/10.1016/j.jenvman.2016.03.012, 2016.

Diao, H., Wang, A., Yang, H., Yuan, F., Guan, D., and Wu, J.: Responses of evapotranspiration to droughts across global forests: A systematic assessment, Can. J. For. Res., 51, 1–9, https://doi.org/10.1139/cjfr-2019-0436, 2021.

Erler, A. R., Frey, S. K., Khader, O., d'Orgeville, M., Park, Y. J., Hwang, H. T., Lapen, D. R., Richard Peltier, W., and Sudicky, E. A.: Simulating Climate Change Impacts on Surface Water Resources Within a Lake-Affected Region Using Regional Climate Projections, Water Resour. Res., 55, 130–155, https://doi.org/10.1029/2018WR024381, 2019.

Falkenmark, M. and Rockström, J.: Building Water Resilience in the Face of Global Change: From a Blue-Only to a

466   Green-Blue Water Approach to Land-Water Management, J. Water Resour. Plan. Manag., 136, 606–610,
467   https://doi.org/10.1061/(asce)wr.1943-5452.0000118, 2010.

468   Foster, S. S. D. and Chilton, P. J.: Groundwater: The processes and global significance of aquifer degradation, Philos.
469   Trans. R. Soc. B Biol. Sci., 358, 1957–1972, https://doi.org/10.1098/rstb.2003.1380, 2003.

470   Griebler, C. and Avramov, M.: Groundwater ecosystem services: A review, Freshw. Sci., 34, 355–367,
471   https://doi.org/10.1086/679903, 2015.

472   Hogg, E. H.: Temporal scaling of moisture and the forest-grassland boundary in western Canada, Agric. For.
473   Meteorol., 84, 115–122, https://doi.org/10.1016/S0168-1923(96)02380-5, 1997.

474   Honeck, E., Gallagher, L., von Arx, B., Lehmann, A., Wyler, N., Villarrubia, O., Guinaudeau, B., and Schlaepfer, M.
475   A.: Integrating ecosystem services into policymaking – A case study on the use of boundary organizations, Ecosyst.
476   Serv., 49, https://doi.org/10.1016/j.ecoser.2021.101286, 2021.

477   Hosen, J. D., Aho, K. S., Appling, A. P., Creech, E. C., Fair, J. H., Hall, R. O., Kyzivat, E. D., Lowenthal, R. S., Matt,
478   S., Morrison, J., Saiers, J. E., Shanley, J. B., Weber, L. C., Yoon, B., and Raymond, P. A.: Enhancement of primary
479   production during drought in a temperate watershed is greater in larger rivers than headwater streams, Limnol.
480   Oceanogr., 64, 1458–1472, https://doi.org/10.1002/lno.11127, 2019.

481   Jin, Z., Liang, W., Yang, Y., Zhang, W., Yan, J., Chen, X., Li, S., and Mo, X.: Separating Vegetation Greening and
482   Climate Change Controls on Evapotranspiration trend over the Loess Plateau, Sci. Rep., 7, 1–15,
483   https://doi.org/10.1038/s41598-017-08477-x, 2017.

484   L'Ecuyer-Sauvageau, C., Dupras, J., He, J., Auclair, J., Kermagoret, C., and Poder, T. G.: The economic value of
485   Canada's National Capital Green Network, PLoS One, 16, 1–29, https://doi.org/10.1371/journal.pone.0245045, 2021.

486   Li, Q., Qi, J., Xing, Z., Li, S., Jiang, Y., Danielescu, S., Zhu, H., Wei, X., and Meng, F. R.: An approach for assessing
487   impact of land use and biophysical conditions across landscape on recharge rate and nitrogen loading of groundwater,
488   Agric. Ecosyst. Environ., 196, 114–124, https://doi.org/10.1016/j.agee.2014.06.028, 2014.

489   Liu, Y. and El-Kassaby, Y. A.: Evapotranspiration and favorable growing degree-days are key to tree height growth
490   and ecosystem functioning: Meta-Analyses of Pacific Northwest historical data, 1st Annu. IEEE Conf. Control
491   Technol. Appl. CCTA 2017, 2017-Janua, 7–12, https://doi.org/10.1038/s41598-018-26681-1, 2017.

492   Liu, Y., Zhou, R., Wen, Z., Khalifa, M., Zheng, C., Ren, H., Zhang, Z., and Wang, Z.: Assessing the impacts of
493   drought on net primary productivity of global land biomes in different climate zones, Ecol. Indic., 130, 108146,
494   https://doi.org/10.1016/j.ecolind.2021.108146, 2021.

495   Logan, C., Cummings, D. I., Pullan, S., Pugin, A., Russell, H. A. J., and Sharpe, D. R.: Hydrostratigraphic model of
496   the South Nation watershed region, south-eastern Ontario, Geological Survey of Canada, 17 pp.,
497   https://doi.org/https://doi.org/10.4095/248203, 2009.

498   Loheide, S. P.: A method for estimating subdaily evapotranspiration of shallow groundwater using diurnal water table
499   fluctuations, Ecohydrology, 1, 59–66, 2008.

500   Lowe, B. H., Zimmer, Y., and Oglethorpe, D. R.: Estimating the economic value of green water as an approach to
501   foster the virtual green-water trade, Ecol. Indic., 136, 108632, https://doi.org/10.1016/j.ecolind.2022.108632, 2022.

502   Mammola, S., Cardoso, P., Culver, D. C., Deharveng, L., Ferreira, R. L., Fišer, C., Galassi, D. M. P., Griebler, C.,

503 Halse, S., Humphreys, W. F., Isaia, M., Malard, F., Martinez, A., Moldovan, O. T., Niemiller, M. L., Pavlek, M.,

504 Reboleira, A. S. P. S., Souza-Silva, M., Teeling, E. C., Wynne, J. J., and Zagmajster, M.: Scientists' warning on the

505 conservation of subterranean ecosystems, Bioscience, 69, 641–650, https://doi.org/10.1093/biosci/biz064, 2019.

506 McKenney, D. W., Hutchiinson, M. F., Papadopol, P., Lawrence, K., Pedlar, J., Campbell, K., Milewska, E.,

507 Hopkinson, R. F., Price, D., and Owen, T.: Customized spatial climate models for North America, Bull. Am. Meteorol.

508 Soc., 92, 1611–1622, https://doi.org/10.1175/2011BAMS3132.1, 2011.

509 Millenium Ecosystem Assessment (MEA): Ecosystems and Human Well-Being: Synthesis, Island Press, 285 pp.,

510 https://doi.org/10.1057/9780230625600, 2005.

511 Miller, S. A. and Lyon, S. W.: Tile Drainage Increases Total Runoff and Phosphorus Export During Wet Years in the

512 Western Lake Erie Basin, 3, 1–13, https://doi.org/10.3389/frwa.2021.757106, 2021.

513 Moriasi, D. N., Arnold, J. G., Van Liew, M. W., Bingner, R. L., Harmel, R. D., and Veith, T. L.: Model evaluation

514 guidelines for systematic quantification of accuracy in watershed simulations, Trans. ASABE, 50, 885–900,

515 https://doi.org/10.13031/2013.23153, 2007.

516 Muñoz-Sabater, J., Dutra, E., Agustí-Panareda, A., Albergel, C., Arduini, G., Balsamo, G., Boussetta, S., Choulga,

517 M., Harrigan, S., Hersbach, H., Martens, B., Miralles, D. G., Piles, M., Rodríguez-Fernández, N. J., Zsoter, E.,

518 Buontempo, C., and Thépaut, J. N.: ERA5-Land: A state-of-the-art global reanalysis dataset for land applications,

519 Earth Syst. Sci. Data, 13, 4349–4383, https://doi.org/10.5194/essd-13-4349-2021, 2021.

520 MYD15A2H MODIS/Aqua Leaf Area Index/FPAR 8-Day L4 Global 500m SIN Grid. NASA LP DAAC:

521 Neff, B. P., Day, S. M., Piggott, A. R., and Fuller, L. M.: Base flow in the Great Lakes basin, U.S. Geol. Surv. Sci.

522 Investig. Rep., 32, 2005.

523 Ochoa, V. and Urbina-Cardona, N.: Tools for spatially modeling ecosystem services: Publication trends, conceptual

524 reflections and future challenges, Ecosyst. Serv., 26, 155–169, https://doi.org/10.1016/j.ecoser.2017.06.011, 2017.

525 Ontario Geological Survey: Surficial Geology of Southern Ontario, Miscellaneous Release--Data 128-REV. Ontario

526 Geological Survey., 1–7 pp., 2010.

527 Ontario Integrated Hydrology Data: Elevation and mapped water features for provincial scale hydrology applications:

528 https://geohub.lio.gov.on.ca/maps/mnrf::ontario-integrated-hydrology-oih-data/about.

529 Qiu, J., Zipper, S. C., Motew, M., Booth, E. G., Kucharik, C. J., and Loheide, S. P.: Nonlinear groundwater influence

530 on biophysical indicators of ecosystem services, Nat. Sustain., 2, 475–483, https://doi.org/10.1038/s41893-019-0278-

531 2, 2019.

532 Richardson, M. and Kumar, P.: Critical Zone services as environmental assessment criteria in intensively managed

533 landscapes, Earth's Futur., 5, 617–632, https://doi.org/10.1002/2016EF000517, 2017.

534 Schaap, M. G., Leij, F. J., and Van Genuchten, M. T.: Rosetta: A computer program for estimating soil hydraulic

535 parameters with hierarchical pedotransfer functions, J. Hydrol., 251, 163–176, https://doi.org/10.1016/S0022-

536 1694(01)00466-8, 2001.

537 Schyns, J. F., Hoekstra, A. Y., Booij, M. J., Hogeboom, R. J., and Mekonnen, M. M.: Limits to the world's green

538 water resources for food, feed, fiber, timber, and bioenergy, Proc. Natl. Acad. Sci. U. S. A., 116, 4893–4898,

539 https://doi.org/10.1073/pnas.1817380116, 2019.

540 Siebert, S., Burke, J., Faures, J. M., Frenken, K., Hoogeveen, J., Döll, P., and Portmann, F. T.: Groundwater use for

541 irrigation - A global inventory, Hydrol. Earth Syst. Sci., 14, 1863–1880, https://doi.org/10.5194/hess-14-1863-2010,

542 2010.

543 SLC: Soil Landscapes of Canada Version 3.2, 2007–2008 pp., 2010.

544 Su, Y., Feng, Q., Zhu, G., Wang, Y., and Zhang, Q.: A New Method of Estimating Groundwater Evapotranspiration

545 at Sub-Daily Scale Using Water Table Fluctuations, Water (Switzerland), 14, 1–14,

546 https://doi.org/10.3390/w14060876, 2022.

547 Sun, B., Zhao, H., and Wang, X.: Effects of drought on net primary productivity: Roles of temperature, drought

548 intensity, and duration, Chinese Geogr. Sci., 26, 270–282, https://doi.org/10.1007/s11769-016-0804-3, 2016.

549 Sun, G., Hallema, D., and Asbjornsen, H.: Ecohydrological processes and ecosystem services in the Anthropocene: a

550 review, Ecol. Process., 6, https://doi.org/10.1186/s13717-017-0104-6, 2017.

551 Tan, S., Wang, H., Prentice, I. C., and Yang, K.: Land-surface evapotranspiration derived from a first-principles

552 primary production model, Environ. Res. Lett., 16, https://doi.org/10.1088/1748-9326/ac29eb, 2021.

553 Taylor, R. G., Scanlon, B., Döll, P., Rodell, M., Van Beek, R., Wada, Y., Longuevergne, L., Leblanc, M., Famiglietti,

554 J. S., Edmunds, M., Konikow, L., Green, T. R., Chen, J., Taniguchi, M., Bierkens, M. F. P., Macdonald, A., Fan, Y.,

555 Maxwell, R. M., Yechieli, Y., Gurdak, J. J., Allen, D. M., Shamsudduha, M., Hiscock, K., Yeh, P. J. F., Holman, I.,

556 and Treidel, H.: Ground water and climate change, Nat. Clim. Chang., 3, 322–329,

557 https://doi.org/10.1038/nclimate1744, 2013.

558 Vigerstol, K. L. and Aukema, J. E.: A comparison of tools for modeling freshwater ecosystem services, J. Environ.

559 Manage., 92, 2403–2409, https://doi.org/10.1016/j.jenvman.2011.06.040, 2011.

560 Wheaton, E., Kulshreshtha, S., Wittrock, V., and Koshida, G.: Dry times: Hard lessons from the Canadian drought of

561 2001 and 2002, Can. Geogr., 52, 241–262, https://doi.org/10.1111/j.1541-0064.2008.00211.x, 2008.

562 Wichelns, D.: Do estimates of water productivity enhance understanding of farm-level water management?, Water

563 (Switzerland), 6, 778–795, https://doi.org/10.3390/w6040778, 2014.

564 Xu, C., Li, Y., Hu, J., Yang, X., Sheng, S., and Liu, M.: Evaluating the difference between the normalized difference

565 vegetation index and net primary productivity as the indicators of vegetation vigor assessment at landscape scale,

566 Environ. Monit. Assess., 184, 1275–1286, https://doi.org/10.1007/s10661-011-2039-1, 2012.

567 Xu, S., Frey, S. K., Erler, A. R., Khader, O., Berg, S. J., Hwang, H. T., Callaghan, M. V., Davison, J. H., and Sudicky,

568 E. A.: Investigating groundwater-lake interactions in the Laurentian Great Lakes with a fully-integrated surface water-

569 groundwater model, J. Hydrol., 594, 125911, https://doi.org/10.1016/j.jhydrol.2020.125911, 2021.

570 Xu, Y. and Xiao, F.: Assessing Changes in the Value of Forest Ecosystem Services in Response to Climate Change

571 in China, Sustain., 14, https://doi.org/10.3390/su14084773, 2022.

572 Yang, H., Luo, P., Wang, J., Mou, C., Mo, L., Wang, Z., Fu, Y., Lin, H., Yang, Y., and Bhatta, L. D.: Ecosystem

573 evapotranspiration as a response to climate and vegetation coverage changes in Northwest Yunnan, China, PLoS One,

574 10, 1–17, https://doi.org/10.1371/journal.pone.0134795, 2015.

575 Yang, X. and Liu, J.: Assessment and valuation of groundwater ecosystem services: A case study of Handan City,

576 China, Water (Switzerland), 12, https://doi.org/10.3390/w12051455, 2020.

577 Zhao, M., Aa, G., Liu, Y., and Konings, A.: Evapotranspiration frequently increases during droughts, Nat. Clim.
578 Chang., 6904, 2022.
579 Zisopoulou, K., Zisopoulos, D., and Panagoulia, D.: Water Economics: An In-Depth Analysis of the Connection of
580 Blue Water with Some Primary Level Aspects of Economic Theory I, Water (Switzerland), 14,
581 https://doi.org/10.3390/w14010103, 2022.
582

583 **Appendix**

584 The annual outputs (ET$_a$, surface water, subsurface water, precipitation and outflow) from the HGS model are given

585 in Table 1A.

Table A1: HGS outputs from the SNW simulation

Year	ET$_a$ (m³)	Surface water (m³)	Subsurface water (m³)	Precipitation (m³)	Outflow (m³)	Surface evaporation (m³)	Subsurface evaporation (m³)	Subsurface transpiration (m³)
2000	2,085,534,445	69,424,628	222,709,069,460	4,199,527,096	76,327,719	75,020,473	184,374,990	945,999,818
2001	2,477,004,097	54,513,422	222,240,461,950	3,003,497,233	32,382,847	49,049,150	193,684,126	1,525,263,969
2002	2,309,984,877	61,588,887	222,788,771,412	3,598,706,939	50,743,315	49,496,381	137,246,184	150,943,1,700
2003	2,264,696,091	68,998,342	222,524,086,305	4,253,877,105	64,623,628	63,041,934	155,345,628	1,263,073,935
2004	2,197,974,479	67,358,376	222,569,571,666	3,631,932,688	47,291,949	56,472,059	186,217,551	1,224,545,264
2005	2,416,958,064	67,153,617	222,566,818,892	3,988,298,138	48,434,304	62,293,999	203,745,742	1407,718,083
2006	2,293,950,204	74,422,486	222,666,754,361	4,538,849,536	77,813,027	73,310,604	176,406,194	1,175,390,417
2007	2,385,260,383	65,967,543	222,611,557,149	3,679,748,277	47,306,909	55,442,956	193,054,015	1,352,247,667
2008	2,236,139,918	79,130,070	222,736,726,608	5,070,858,236	75,918,796	63,243,999	153,505,172	1,001,912,242
2009	2,142,956,266	72,673,133	222,733,824,127	3,753,041,839	73,573,865	74,320,182	175,808,767	1,034,718,786
2010	2,450,480,102	67,043,193	222,626,541,197	3,686,832,140	67,076,288	78,166,506	204,928,373	1,337,194,629
2011	2,398,275,129	63,710,702	222,487,837,813	3,743,641,761	47,912,738	56,432,877	170,459,783	1,404,943,119

2012	2,589,094,745	52,013,667	222,334,569,769	2,864,258,811	26,234,849	58,974,276	223,348,145	1,633,465,101
2013	2,269,228,484	64,978,113	222,458,625,710	3,700,833,331	54,270,475	67,961,698	205,253,614	1,227,712,022
2014	2,193,041,030	69,944,514	222,574,462,508	3,974,971,693	44,803,342	67,115,318	170,740,982	1,220,179,455
2015	2,449,702,370	62,201,787	222,466,595,816	3,374,434,139	14,781,188	64,640,268	227,937,634	1,407,052,424
2016	2,516,780,613	59,120,794	222,402,665,868	3,747,442909	40,697,558	53,448,526	220,313,313	1,610,087,162
2017	2,273,903,311	80,775,412	222,688,809,435	5,228,987,865	63,739,372	77,841,432	192,369,477	1,176,497,385

590   The SNW has approximately 110 m of vertical relief from its highest point in the southwest corner to its outlet at the Ottawa

River at its northern most point (Fig. 1A).
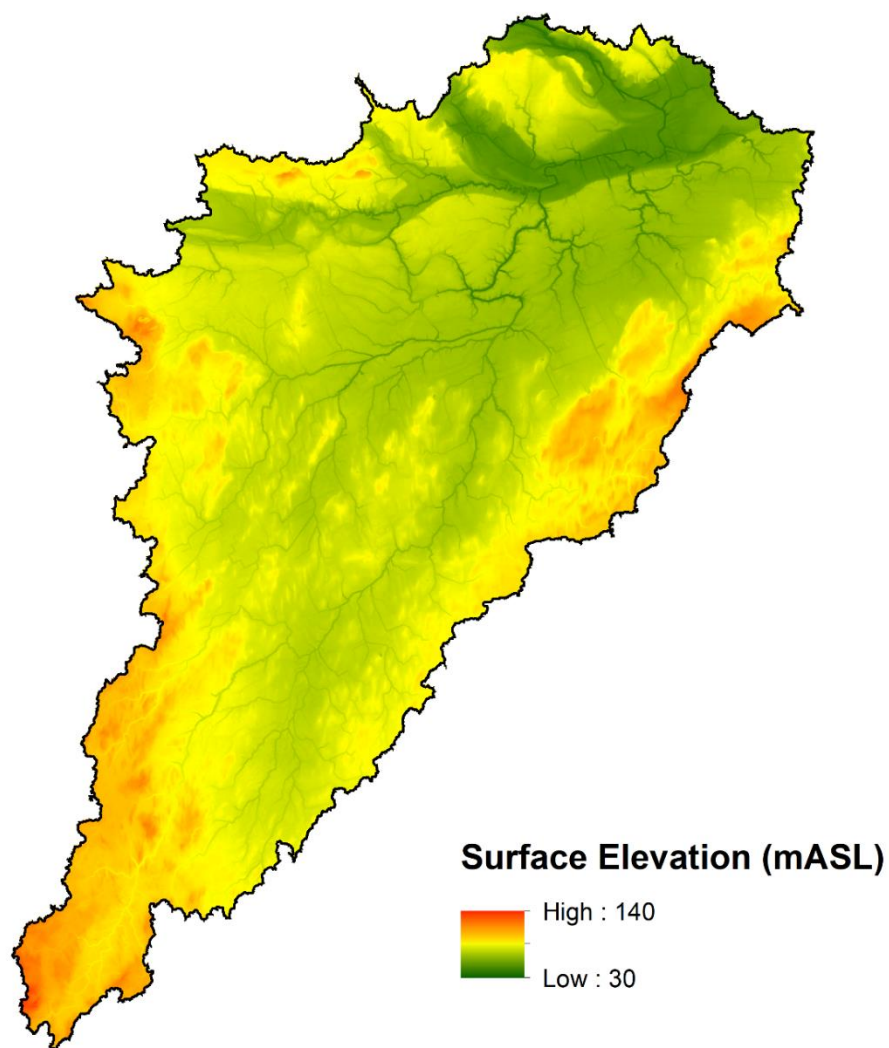
Figure 1A: Land surface elevation of the SNW

595
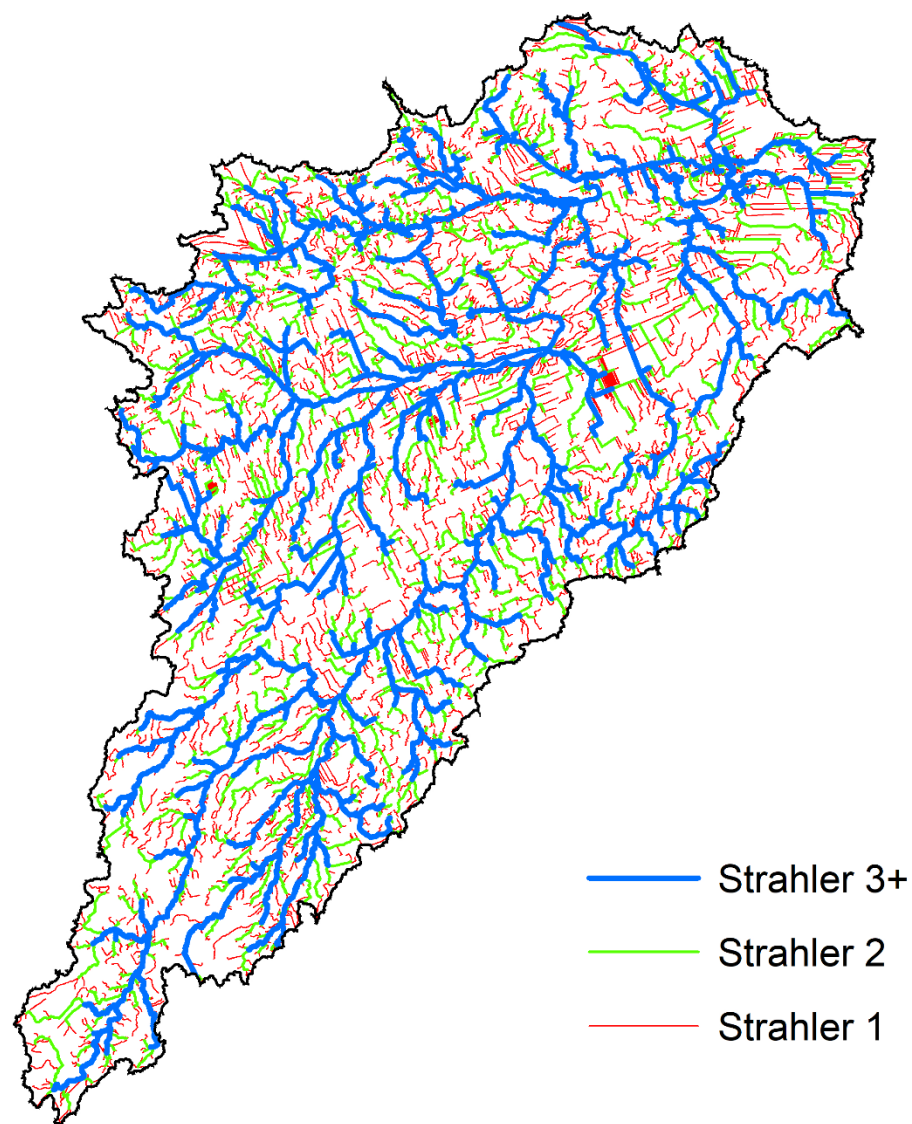
Figure 2A. Stream network distribution across the South Nation watershed, consisting of 1606 km of Strahler 3+ streams, 1548 km of Strahler 2 streams, and 3335 km of Strahler 1 streams(Ontario Ministry of Natural Resources and Forestry 2013).
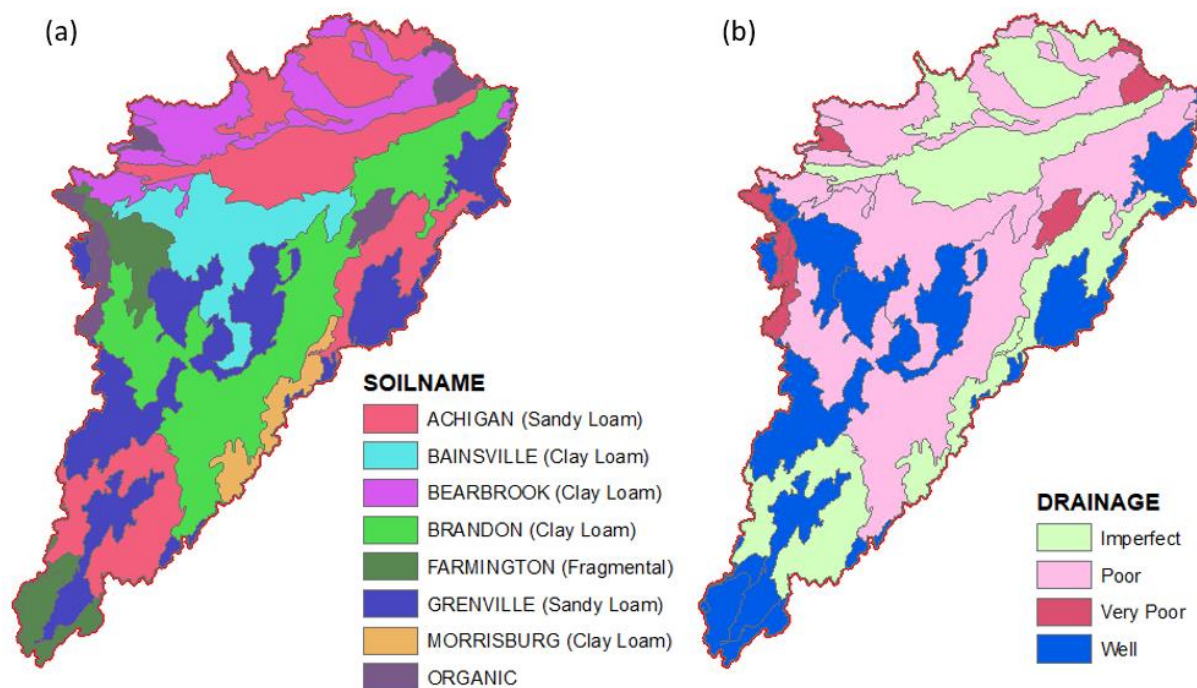
600   Figure 3A. (a) Soil distribution, and (b) soil drainage status across the South Nation watershed.
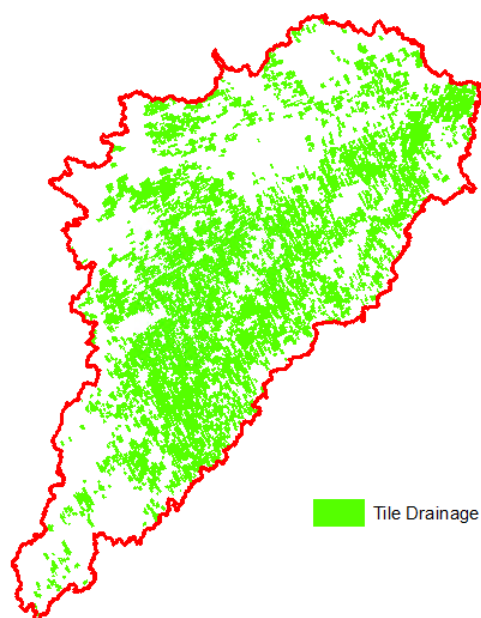
Figure 4A. Tile drainage distribution across the South Nation watershed (data provided by South Nation Conservation

Authority).
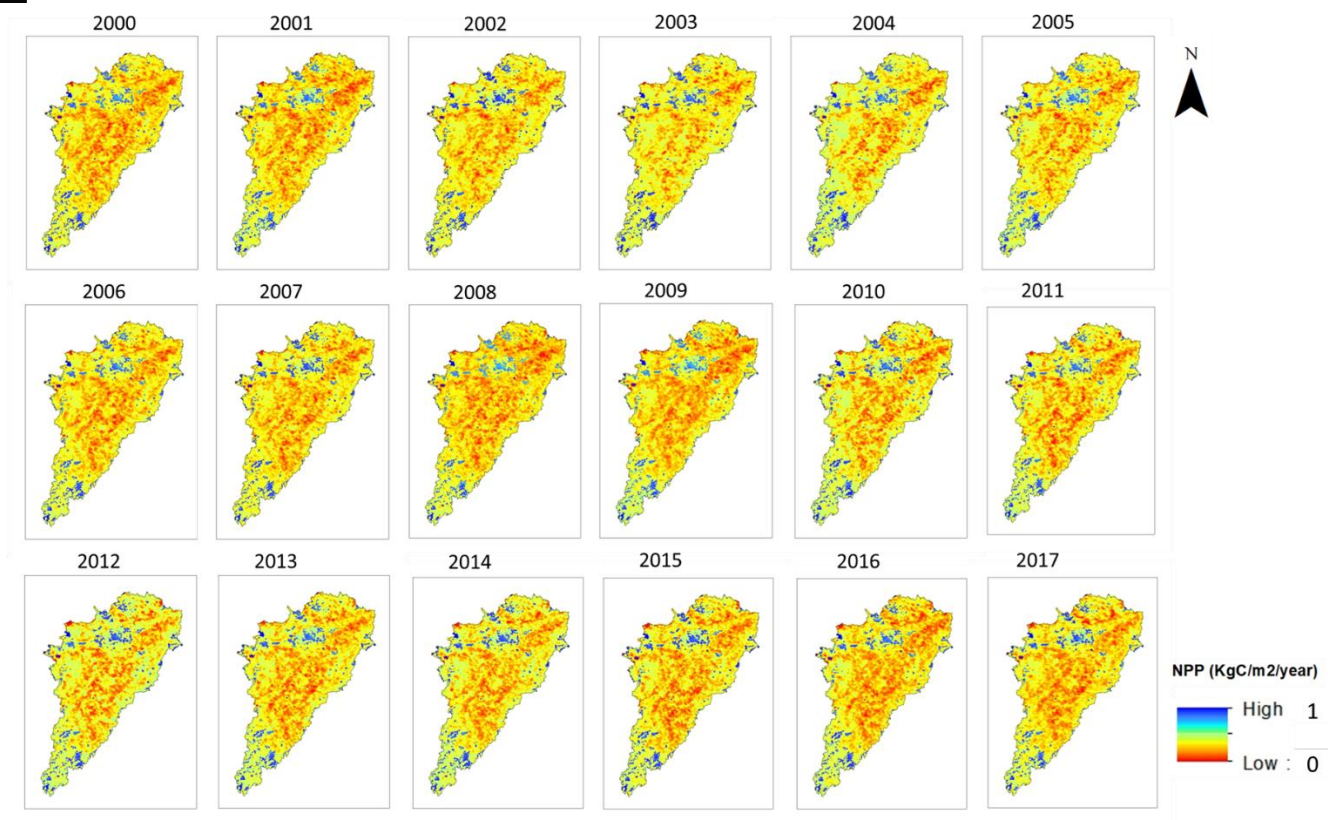
605   Figure 5A: Net Primary Productivity (NPP) data for SNW (based on MODIS data).